

Cholesterol-binding molecules MLN64 and ORP1L mark distinct late endosomes with transporters ABCA3 and NPC1[§]

Rik van der Kant, Ilse Zondervan, Lennert Janssen, and Jacques Neefjes¹

Division of Cell Biology, Netherlands Cancer Institute, Amsterdam, Netherlands

Abstract Cholesterol is an essential lipid in eukaryotic cells and is present in membranes of all intracellular compartments. A major source for cellular cholesterol is internalized lipoprotein particles that are transported toward acidic late endosomes (LE) and lysosomes. Here the lipoprotein particles are hydrolyzed, and free cholesterol is redistributed to other organelles. The LE can contain over half of the cellular cholesterol and, as a major sorting station, can contain many cholesterol-binding proteins from the ABCA, STARD, and ORP families. Here, we show that metastatic lymph node 64 (MLN64, STARD3) and oxysterol-binding protein-related protein 1L (ORP1L) define two subpopulations of LE. MLN64 is present on a LE containing the cholesterol transporter ABCA3, whereas ORP1L localizes to another population of LE containing Niemann Pick type C1 (NPC1), a cholesterol exporter. Endocytosed cargo passes through MLN64/ABCA3-positive compartments before it reaches ORP1L/NPC1-positive LE. The MLN64/ABCA3 compartments cycle between LE and plasma membrane and frequently contact “later” ORP1L/NPC1-containing LE. We propose two stages of cholesterol handling in late endosomal compartments: first, cholesterol enters MLN64/ABCA3-positive compartments from where it can be recycled to the plasma membrane, and later, cholesterol enters ORP1L/NPC1 endosomes that mediate cholesterol export to the endoplasmic reticulum.—van der Kant, R., I. Zondervan, L. Janssen, and J. Neefjes. Cholesterol-binding molecules MLN64 and ORP1L mark distinct late endosomes with transporters ABCA3 and NPC1. *J. Lipid Res.* 2013. 54: 2153–2165.

Supplementary key words lysosome • metastatic lymph node 64 • oxysterol-binding protein-related protein 1L • ATP binding cassette transporter A3 • Niemann Pick disease type C1 • STARD3

Cholesterol is a key component of cellular membranes and is essential for the regulation of membrane rigidity, cellular compartmentalization, enzyme function, and the production of steroid hormones (1). A major source of cellular cholesterol is the endocytosis of lipoproteins from

the cell surface and subsequent processing of these particles in late endosomal (LE) and lysosomal compartments. At the plasma membrane of cells, low-density lipoprotein receptors (LDLR) internalize lipoprotein particles by clathrin-coated endocytosis. These lipoprotein particles, including VLDL and LDL, are a major source of cholesterol in most cells. After initial endocytosis, the lipoproteins are transported toward acid LE compartments where cholesteryl esters are hydrolyzed by acid lipases to generate free unesterified cholesterol (1). This free cholesterol can subsequently be transferred to other compartments, such as recycling endosomes, the endoplasmic reticulum (ER), the plasma membrane (PM), and mitochondria (1–4). Late (multivesicular) endosomes can contain over half of the total cellular cholesterol content (5), and many cholesterol-binding proteins localize to these compartments to control the flow of intercellular cholesterol. How the functions of these proteins relate to each other and how they communicate to distribute the LE cholesterol to other compartments is unclear. Metastatic lymph node 64 (MLN64), also known as STARD3, is a lipid-binding protein from the steroidogenic acute regulatory protein (StAR)-related lipid transfer domain (START) protein family with two functional domains: a C-terminal domain containing the START domain that projects into the cytoplasm and an N-terminal 4-transmembrane domain (6). MLN64 is reported to be involved in the egress of cholesterol from LE to mitochondria (4, 7), and it regulates late endosomal tethering and fusion dynamics involving actin (8). Another cholesterol-binding protein that controls LE dynamics is the oxysterol-binding protein-related protein 1L (ORP1L). ORP1L is recruited to LE membranes by binding to the small GTPase RAB7, and it is part of a tripartite

Abbreviations: ER, endoplasmic reticulum; LE, late endosomal; MLN64, metastatic lymph node 64; NPC1, Niemann Pick type C1; ORP1L, oxysterol-binding protein-related protein 1L; PM, plasma membrane; RILP, RAB7-interacting lysosomal protein.

¹To whom correspondence should be addressed.

e-mail: j.neefjes@nki.nl

[§]The online version of this article (available at <http://www.jlr.org>) contains supplementary data in the form of four figures and three movies.

This work was supported by grants from de Nederlandse organisatie voor Wetenschappelijk Onderzoek (NWO-TOP) and the European Research Council.

Manuscript received 28 February 2013 and in revised form 22 May 2013.

Published, *JLR Papers in Press*, May 26, 2013

DOI 10.1194/jlr.M037325

Copyright © 2013 by the American Society for Biochemistry and Molecular Biology, Inc.

This article is available online at <http://www.jlr.org>

complex of RAB7, RAB7-interacting lysosomal protein (RILP), and ORP1L that regulates recruitment of the dynein motor and the homotypic fusion and vacuole protein sorting (HOPS) complex to late endosomes and thereby minus-end transport and tethering (9–12). Although ORP1L is probably not directly involved in shuttling cholesterol out of the LE, it is able to sense the amount of cholesterol on the cytosolic face of the LE-limiting membrane and induces contact sites between LE and the ER to control binding of the dynein motor and the HOPS complex to RAB7-RILP (10, 12). Cholesterol levels thus control positioning and tethering of LE. Another protein associating with the RAB7-RILP complex that controls LE transport is neuronal ceroid lipofuscinosis protein CLN3. When mutated, this protein causes classical juvenile onset neuronal ceroid lipofuscinosis, a fatal inherited neurodegenerative lysosomal storage disorder in which lipopigments accumulate in lysosomes (13). Proteins of the ATP binding cassette class A (ABCA) proteins have recently been shown to be present in LE compartments due to a conserved targeting motif (14). ABCA proteins are transporters that use ATP to drive translocation of various substrates, including lipids, across membranes. ABCA3 probably functions as lipid pump for the translocation of phospholipids and cholesterol into lysosomal-like organelles (lamellar bodies) (15). The different cholesterol-binding proteins on late endosomes are likely involved in different steps of cholesterol transport and handling, and different diseases are associated with these molecules. Mutations in ABCA3 cause fatal respiratory distress syndrome in newborns, probably due to a defect in lamellar body biogenesis where exocytosis is required for the formation of the lipid surface-lining layer of the alveolar epithelium of lungs (15). Cholesterol egress from the LE into the ER requires proteins such as Niemann Pick type C protein 1 (NPC1) and NPC2, which transfer cholesterol from the lumen of the LE into the LE-limiting membrane (16, 17). Mutations in the Niemann Pick type C proteins cause a fatal, neurodegenerative disorder in which cholesterol accumulates in LE and disturbs transport when the altered cholesterol content is sensed by ORP1L (10).

How cholesterol is transferred from the LE to the ER is debated. Cholesterol could be directly transferred from the LE to the ER (18) possibly mediated by an ER-resident protein of the oxysterol-binding protein family (ORP5) (19). However, only about 30% LE cholesterol is directly transported from LE to the ER, whereas 70% passes through the plasma membrane prior to esterification in the ER (2). LE cholesterol is rapidly moved toward the plasma membrane, whereas reesterification in the ER shows a 0.5–1 h lag, arguing against direct LE to ER movement of cholesterol (3). MLN64 has been shown to egress cholesterol from LE to mitochondria even in the absence of functional Niemann-Pick type C1 proteins (4, 7).

Apart from these findings, little is known about the exact localization and cross-talk between the different cholesterol sensing and transferring proteins on the LE. Here, we address the location of MLN64 in relation to ORP1L. We show that MLN64 and ORP1L define two distinct LE

compartments. Whereas MLN64 is present in “early” ABCA3-positive LE compartments, ORP1L defines a population of “late” late endosomes labeled by the cholesterol transporter NPC1. The subcompartments possibly reflect sites where LE cholesterol is handled differently to ensure proper cellular homeostasis of this essential and complex hydrophobic molecule.

EXPERIMENTAL PROCEDURES

Reagents

Rabbit anti-GFP and rabbit anti-mRFP antibodies were generated in-house using purified His-mRFP and His-GFP recombinant proteins, respectively. The rabbit-anti MLN64 serum was generated in-house using purified His-START domain of human MLN64. Other antibodies used were anti-NPC1 (Novus Biologicals), rabbit anti-ORP1L (gift from V. Olkkonen, National Public Health Institute, Helsinki, Finland), mouse anti-CD63 (20), mouse monoclonal anti-EEA1 (BD Biosciences), anti-HA (Roche), anti-EEA1 (BD Biosciences), anti-M6PR (Affinity Bioreagents), and anti-NPC1 (BD Biosciences).

Cell culture

MeJJuSo cells were cultured in Iscove's modified Dulbecco's medium (IMDM; Invitrogen) supplemented with 8% FCS. SKBR3 cells were cultured in Dulbecco's modified Eagle medium (DMEM) supplemented with 8% FCS in a 5% CO₂-humidified culture hood at 37°C.

Microscopy

Transfected cells were fixed 24 h posttransfection with 4% formaldehyde in PBS for 30 min and permeabilized for 5 min with 0.05% Triton X-100 in PBS at room temperature. Nonspecific binding of antibodies was blocked by 0.5% BSA in PBS for 40 min, after which cells were incubated with primary antibodies in 0.5% BSA in PBS for 1 h at room temperature. Bound primary antibodies were visualized with Alexa-Fluor secondary antibody conjugates (Invitrogen). Cells were mounted in Vectashield mounting medium (Vector Laboratories). For methanol fixation, cells were fixed for 5 min in ice-cold methanol, subsequently blocked by 0.5% BSA in PBS for 40 min, and treated similar to the formaldehyde-fixed samples. All specimens were analyzed by confocal laser-scanning microscopes (TCS-SP1, TCS-SP2, or AOBSS; Leica) equipped with HCX Plan-Apochromat 63× NA 1.32 and HCX Plan-Apochromat lbd.bl 63× NA 1.4 oil-corrected objective lenses (Leica). The acquisition software used was LCS (Leica).

Constructs and cloning

RILP and ORP1L constructs have been described previously (9, 10, 21). YFP-MLN-64 was a kind gift from Dr. F. Alpy (Département de Pahtologie Moléculaire, Insitut de Genetique et de Biologie Moleculaire et Cellulaire, Communauté Urbaine de Strasbourg, France). YFP-MLN64 M307R, N311D was generated using site-directed mutagenesis and was sequence verified.

Ovalbumin and LDL uptake and transport

Cells transfected with ORP1L, Δ ORD, Δ ORDPHDPHD, MLN64, or combinations of these were incubated at 37°C with Alexa647-conjugated ovalbumin (Molecular Probes) or DiI-LDL (Molecular Probes, final concentration 20 μ g/ml) in serum-free medium for 20 min. After washing, cells were cultured, fixed after various culturing times, and then analyzed as described.

Image quantification

To measure MLN64 accumulation at the plasma membrane, a region of interest (vector) was drawn over cells and a histogram showing the intensity over the vector was generated in ImageJ. For the other figures, the Manders M1 and M2 coefficients (the percentage of channel A that colocalizes with channel B and reverse) were calculated using the JaCoP plugin in ImageJ.

RESULTS

Localization of endogenous MLN64 on late endosomal compartments and the plasma membrane

To study the endogenous localization of MLN64, we generated a rabbit anti-serum antibody against the C-terminal START domain of human MLN64. This anti-serum recognized MLN64 by WB (Fig. 1A); human MLN64 has a predicted molecular weight of 49 kDa. Expression levels of MLN64 are reported to be similar in most tissues, with the exception of higher expression in lung and blood cells (8, 22). We were unable to detect significant endogenous MLN64 in HeLa and MeJuSo cells, but we could detect endogenous MLN64 in the breast cancer cell line SKBR3 in which MLN64 is amplified. To study the localization of MLN64, we fixed untransfected and MLN64-YFP-transfected SKBR3 cells with paraformaldehyde (PFA), permeabilized cells with Triton-X100, and stained for MLN64 using our antibody. Our antibody recognized high levels of MLN64 in MLN64-YFP-transfected cells (Fig. 1B). In untransfected cells, endogenous MLN64 showed a vesicular staining pattern in addition to a nuclear background staining. Vesicular staining was not observed when cells were stained with preimmune serum (supplementary Fig. 1). Previous studies employing tagged MLN64 revealed that MLN64 is a late endosomal protein (4, 6–8). We confirmed the localization of endogenous MLN64 at CD63-marked late endosomes (Fig. 1C). MLN64 was absent from early endosomes (EEA1 labeled) or mannose-6-phosphate-receptor (M6PR)-positive vesicles (Fig. 1C). Fixation and permeabilization can affect epitope accessibility (23). As an alternative for PFA/Triton-X100 fixation, methanol can also be used. Under these conditions, we again observed a vesicular staining of MLN64 that colocalized with CD63. In addition, we detected staining for MLN64 at the plasma membrane (Fig. 1D). Our data suggest that endogenous MLN64 is present at the plasma membrane and in late endosomes.

MLN64 cycles to the plasma membrane

Although lysosomes are the supposedly end-stage for most cargo internalized from the plasma membrane, many lysosomal proteins are found at the plasma membrane as the result of late endosomal-plasma membrane fusion. These include LE markers, such as CD63 and CD83, which are usually rapidly recycled back to late endosomes by targeting signals in their cytoplasmic tail (24, 25). When we expressed YFP-tagged MLN64 at high levels, we observed a small fraction at the plasma membrane (Fig. 2A). To further

test that MLN64 cycles between the plasma membrane and LE, we blocked endocytosis by expression of dominant-negative (DN) dynamin (26). MLN64 accumulated at the plasma membrane when endocytosis was blocked (Fig. 2B).

ORP1L and MLN64 localize to distinct late endosomal subpopulations

MLN64 is proposed to regulate late endosomal dynamics. Silencing of MLN64 results in dispersion of late endosomes and a delay in degradation of endosomal cargo (8). Another cholesterol-binding protein that controls late endosomal dynamics is ORP1L. ORP1L regulates late endosomal transport by recruiting the ER protein VAP-A, which removes dynein from LE (10). ORP1L also regulates multivesicular body formation (27). As both ORP1L and MLN64 localize to late endosomes, we hypothesized that they could act in assembly to control cholesterol-dependent processes at LE. However, we observed that only a minor fraction of ORP1L and MLN64 colocalized on the same vesicles, whereas the majority of ORP1L and MLN64 localized to different compartments (Fig. 3A). ORP1L was located on (and clustered) small CD63-positive LE, whereas MLN64 was located on other, enlarged LE compartments that also contained the LE marker CD63. In fact, these cholesterol-sensing proteins subdivided the late endosomes. MLN64 and ORP1L vesicles were located adjacent to each other, while colocalization was observed on only a few vesicles. To further study the dynamics of the ORP1L and MLN64 vesicles, we performed live-cell imaging on cells overexpressing ORP1L and MLN64 (supplementary Movie I and Fig. 3B). Again, we observed mutual exclusion of ORP1L and MLN64 on vesicles that closely localized. Vesicles with ORP1L moved together with vesicles containing MLN64 over long distances in the periphery of cells, indicating some sort of interaction or tethering between these vesicles. To further verify these findings, we expressed ORP1L in cells and stained for endogenous MLN64 or expressed MLN64 while staining for ORP1L (supplementary Fig. II). Again a predominant mutual exclusion of closely adjacent vesicles of both types was observed. ORP1L is part of a tripartite complex of RAB7-RILP-ORP1L. As ORP1L and MLN64 are on different vesicles, we wondered whether RILP and MLN64 are also mutually exclusive. Indeed, whereas ORP1L and RILP localized to same vesicles (Fig. 3C, upper panel), RILP and MLN64 localized to different late endosomal subpopulations (Fig. 3C, lower panel). Together, our data suggest that MLN64 and RAB7-RILP-ORP1L localize to distinct late endosomal subpopulations.

Cholesterol-binding ORD domain of ORP1L is involved in spatial separation of ORP1L and MLN64 within late endosomes

ORP1L and MLN64 both contain a cholesterol-sensing domain that can bind cholesterol at the cytosolic site of the late endosomal-limiting membrane. To test whether these domains are important for the mutual exclusion of MLN64 and ORP1L within the late endosomal compartment, we

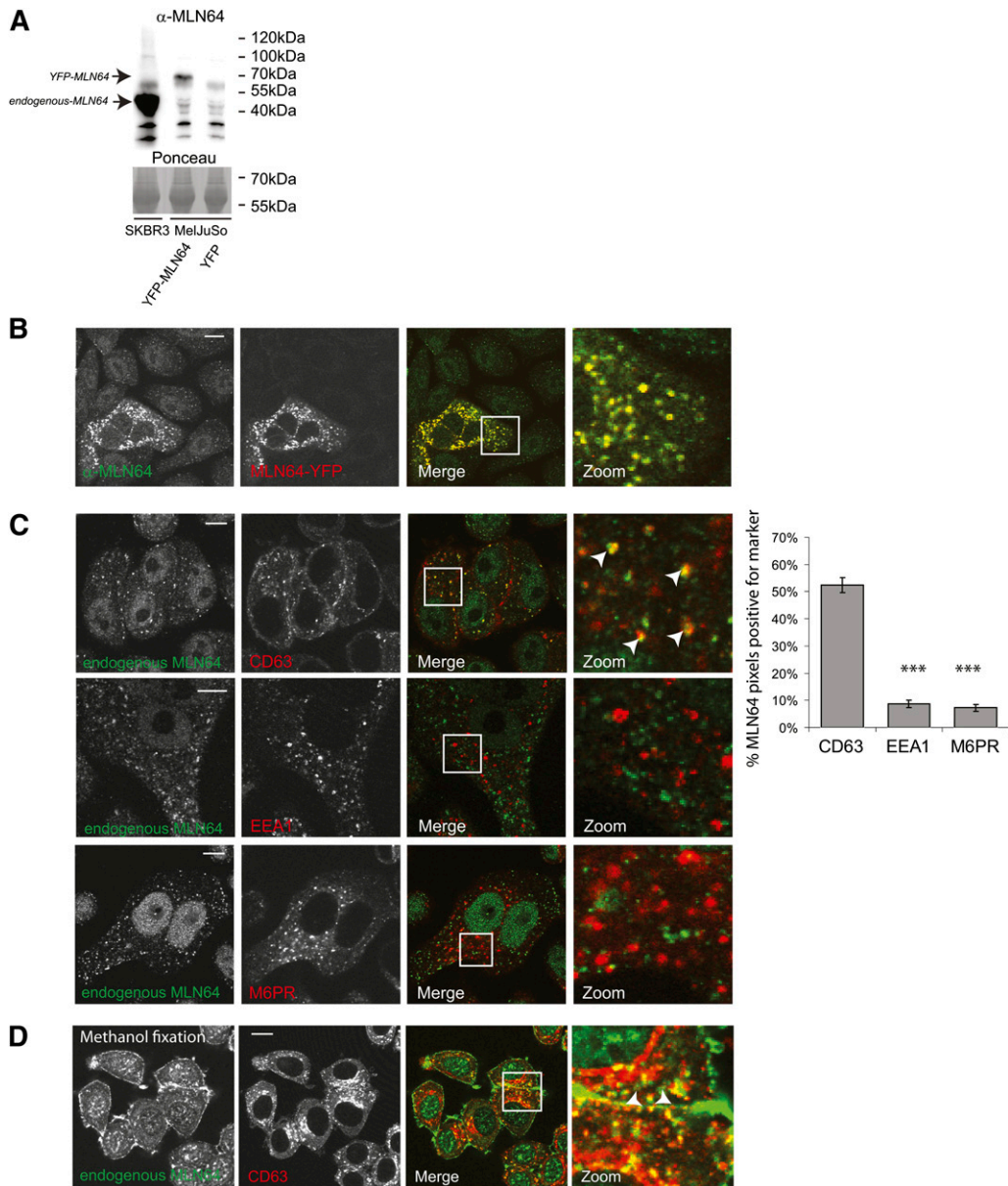


Fig. 1. Endogenous MLN64 on late endosomal compartments and the plasma membrane. (A) Lysates of SKBR3 and MelJuSo cells transfected with YFP-MLN64 or YFP were analyzed by SDS-PAGE and WB before probing with anti-MLN64 antibodies. Position of marker proteins is indicated. (B) SKBR3 cells untransfected (upper cells) or transfected with MLN64-YFP (lower left) were paraformaldehyde (PFA) fixed, permeabilized, and immunolabeled by anti-MLN64 antibodies before imaging by confocal microscopy. Zoom-ins of merged pictures indicated. Scale bar: 10 μ m. $n > 100$. (C) SKBR3 cells were PFA fixed, permeabilized, and stained by anti-MLN64 antibodies (green) and anti-CD63, anti-EEA1, or anti-M6PR antibodies (red) before imaging by confocal microscopy. Zoom-ins of merged pictures indicated. White arrowheads indicate colocalization. Scale bar: 10 μ m. Right panel: Quantification of colocalization using Manders coefficient. Plotted is the percentage of MLN64 signal also positive for the indicated markers. $N > 25$. *** $P < 0.001$. (D) SKBR3 cells were fixed by methanol and stained by anti-MLN64 antibodies (green) and anti-CD63 antibodies (red), and then imaged by confocal microscopy. Zoom-ins of merged pictures indicated. Scale bar: 10 μ m. $n > 100$. White arrowheads indicate plasma membrane location.

expressed proteins with mutations in these domains. The START domain of MLN64 requires two amino acids (M307 and N311) for cholesterol binding; a MLN64(M307R, N311D) mutation has been reported to be deficient in cholesterol binding (8). We verified the late endosomal location of a MLN64(M307R, N311D)-YFP construct (Fig. 4A). Expression of this construct with ORP1L again yielded

mutual exclusion of both proteins within late endosomes (Fig. 4B, upper panel), suggesting that cholesterol binding by the MLN64 START domain is not essential for spatial segregation of MLN64 and ORP1L. We then tested whether the cholesterol-binding ORD domain of ORP1L is involved by coexpressing a truncation mutant of ORP1L missing the ORD domain (ORP1L- Δ ORD) and MLN64.

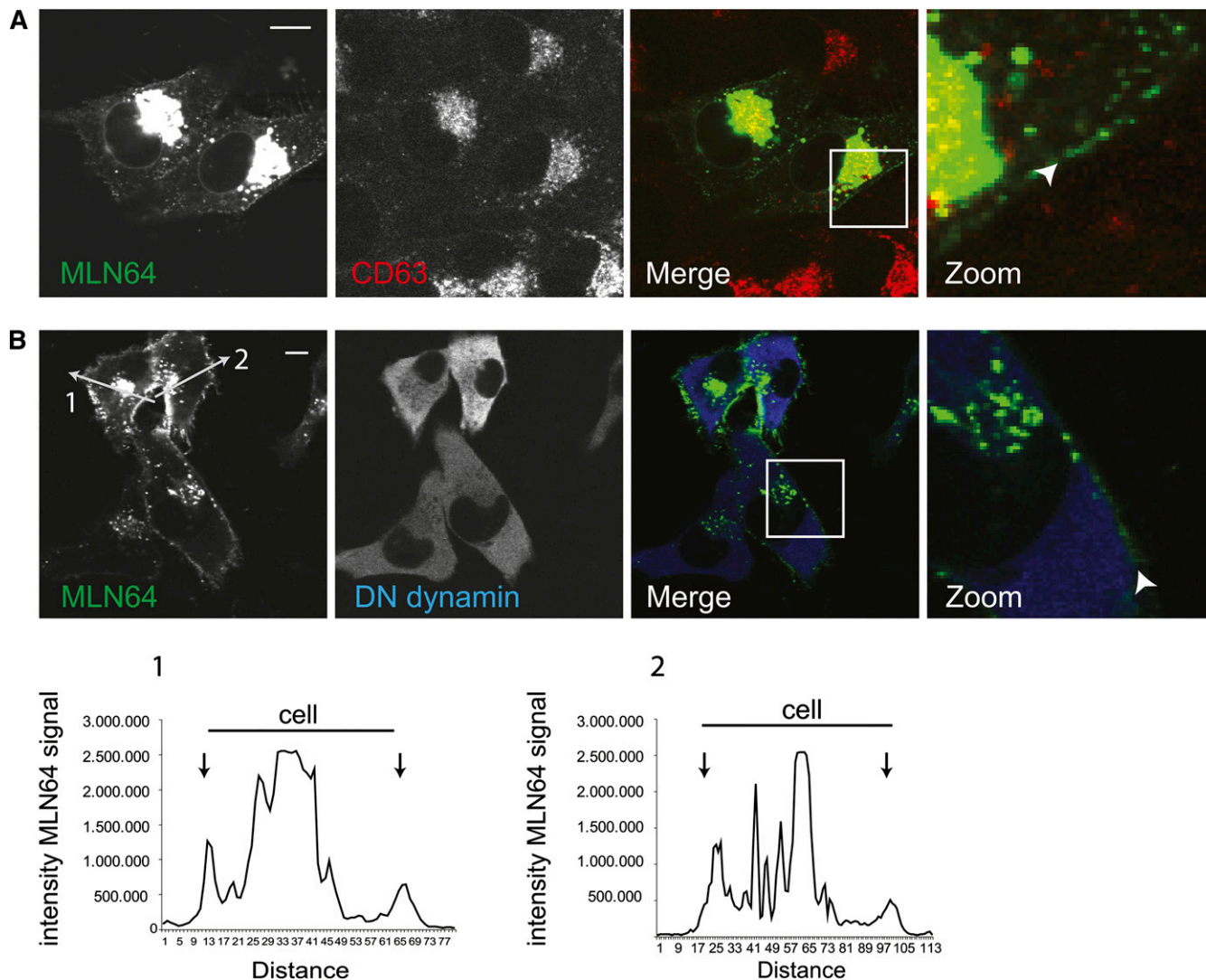


Fig. 2. MLN64 cycles to the plasma membrane. (A) MelJuSo cells overexpressing high levels of MLN64-YFP (indicated MLN64) were immunolabeled by anti-CD63 antibodies and imaged by confocal microscopy. Zoom-ins of merged pictures indicated. Scale bar: 10 μ m. $n > 100$. White arrowheads indicate plasma membrane staining. (B) MelJuSo cells expressing MLN64-YFP in combination with dominant-negative dynamin were PFA fixed, permeabilized, and immunolabeled with anti-dynamin antibodies before imaging by confocal microscopy. Zoom-ins of merged pictures indicated. Scale bar: 10 μ m. $n > 100$. White arrowheads indicate plasma membrane location. Intensity histograms over indicated lines for the MLN64 channel are shown. Black arrows indicate peaks originating from plasma membrane staining at the edge of cells.

Again a predominant exclusion of both proteins within LE could be observed (Fig. 4B, middle panel). However, in about 20% of cells, we observed enlarged vesicles in the periphery of cells that were positive for both MLN64 and ORP1L- Δ ORD. In addition, under these conditions of ORP1L- Δ ORD expression, the MLN64-positive LE clustered (Fig. 4B and supplementary Fig. III). ORP1L has two conformations on the late endosomal membrane: the ORP1L- Δ ORD mutant reflects a cholesterol-unbound conformation, whereas ORP1L- Δ ORDPHDPHD reflects a membrane-bound conformation of the ORD domain, which occurs when LE cholesterol is high (10). Upon coexpression of this ORP1L mutant with MLN64, MLN64 vesicles did not label for ORP1L- Δ ORDPHDPHD. However, most ORP1L- Δ ORDPHDPHD endosomes acquired low levels of MLN64, suggesting fusion and retention of the two

proteins in a fused compartment (Fig. 4B, lower panel). We validated our observations by expressing tagged ORP1L- Δ ORDPHDPHD in SKBR3 cells and staining for endogenous MLN64 (Fig. 4C). Again, MLN64 localized to ORP1L- Δ ORDPHDPHD-positive vesicles. Correct expression at expected molecular weight of all ORP1L and MLN64 mutants was verified by Western blotting (supplementary Fig. IV). Our data indicate that the mutual exclusion of ORP1L and MLN64 within the LE compartment involves the cholesterol-binding domain of ORP1L but not cholesterol binding by the START domain of MLN64.

MLN64 defines an early late endosomal compartment preceding ORP1L-containing late endosomes

If MLN64 and ORP1L define two LE subcompartments, how are these related? We expressed MLN64 and ORP1L

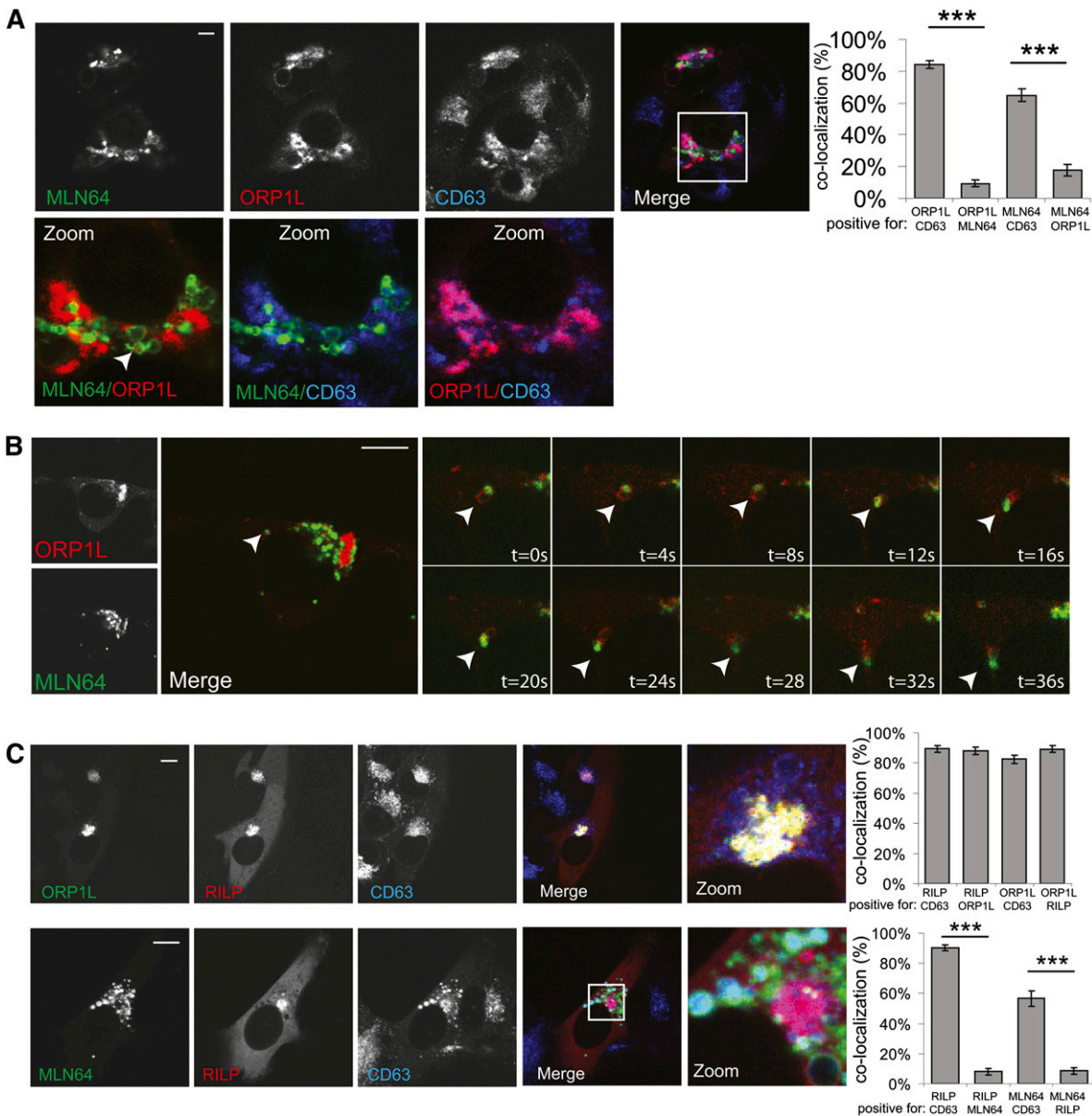


Fig. 3. ORP1L and MLN64 localize to late endosomal subpopulations. (A) MelJuSo cells expressing MLN64-YFP (green) and mRFP-ORP1L (red) were PFA fixed, permeabilized, and immunolabeled with anti-CD63 antibodies (blue) before imaging by confocal microscopy. Zoom-ins of merged pictures indicated. Scale bar: 10 μ m. $n > 100$. White arrowhead indicates a vesicle positive for both MLN64 and ORP1L. Right panel: Quantification of colocalization using Manders coefficient. Plotted is the percentage of signal A that is also positive for signal B for the indicated combinations. $n > 25$, $***P < 0.001$. (B) MelJuSo cells expressing MLN64-YFP (green) and ORP1L-mRFP (red) were imaged by time-lapse confocal microscopy. Merged zoomed snapshots at different time points are shown (right panel). White arrowheads indicate MLN64-positive and ORP1L-positive vesicles interacting over prolonged times. Images correspond to supplementary Movie I. (C) MelJuSo cells expressing ORP1L-GFP and mRFP-RILP (upper panel) or expressing MLN64-YFP (green) and mRFP-RILP (red) (lower panel) were PFA fixed, permeabilized, and immunolabeled with anti-CD63 antibodies (blue) before imaging by confocal microscopy. Zoom-ins of merged pictures indicated. Scale bar: 10 μ m. Right panel: Quantification of colocalization using Manders coefficient. Plotted is the percentage of signal A that is also positive for signal B for the indicated combinations. $n > 25$, $***P < 0.001$.

in cells before feeding cells with fluorescent LDL to study the trafficking of LDL through these compartments (Fig. 5A). At early time points (20 min pulse followed by 30 and 60 min chases), MLN64-positive vesicles acquired the fluorescent LDL (Fig. 5A). At later time points (3 h and 5 h after the original pulse), the LDL accumulated in ORP1L vesicles while the signal decreased in MLN64 vesicles. We repeated these experiments using fluorescent ovalbumin as a fluid-phase endocytosis marker (Fig. 5B). Again at early

time points (20 min pulse followed by 30 and 60 min chases), MLN64-positive vesicles acquired the fluorescent ovalbumin (Fig. 5A, B), while at later time points (3 h and 5 h after the original pulse), the ovalbumin had left the MLN64-positive vesicles and entered ORP1L-positive vesicles. These data suggest that internalized cargo first enters MLN64-containing late endosomal compartments and subsequently enters ORP1L-containing compartments. During live imaging, we again observed extensive cotrafficking

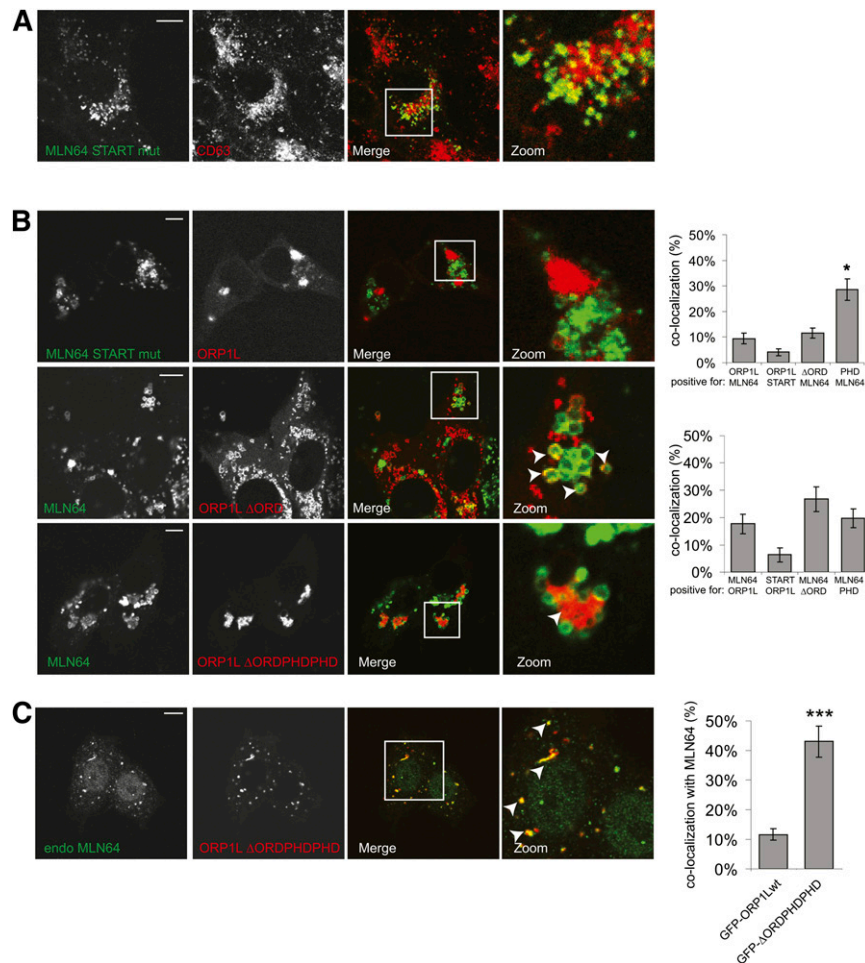


Fig. 4. Role of the cholesterol-binding domain of ORP1L and MLN64 on localization. (A) MeJuSo cells expressing MLN64(M307R, N311D)-YFP were PFA fixed, permeabilized, and immunolabeled with anti-CD63 antibodies (red) before imaging by confocal microscopy. Zoom-ins of merged pictures indicated. Scale bar: 10 μ m. $n > 100$. (B) MeJuSo cells expressing MLN64(M307R, N311D)-YFP (green) and mRFP-ORP1L (red) (upper panel) or expressing YFP-MLN64 (green) together with mRFP-ORP1L- Δ ORD (red) (middle panel) or mRFP-ORP1L- Δ ORDPHDPHD (red) (lower panel) were PFA fixed and imaged by confocal microscopy. Zoom-ins of merged pictures indicated. Scale bar: 10 μ m. Right panels: Quantification of colocalization using Manders coefficient. Plotted is the percentage of signal A that is also positive for signal B for the indicated combinations. $n > 25$. * $P < 0.05$. (C) SKBR3 cells expressing mRFP-ORP1L- Δ ORDPHDPHD (red) were PFA fixed, permeabilized with Triton-X100, stained with an MLN64-antibody, and imaged by confocal microscopy. Zoom-ins of merged pictures indicated. Scale bar: 10 μ m. White arrowheads indicate vesicle positive for both endogenous MLN64 and mRFP-ORP1L- Δ ORDPHDPHD. Right panel: Quantification of colocalization using Manders coefficient. Plotted is the percentage of signal of ORP1Lwt or ORP1L- Δ ORDPHDPHD that is also positive for endogenous MLN64. $n > 25$, *** $P < 0.001$.

of MLN64- and ORP1L-positive vesicles in the cell periphery after 3 h of pulse with fluorescent ovalbumin (Fig. 5C and supplementary Movies II and III). These data also suggest that endocytosed cargo reaches “early” (MLN64-positive) late endosomal compartments that transfer cargo to “later” (ORP1L-positive) late endosomes.

MLN64 and ORP1L localize with different late endosomal cholesterol pumps ABCA3 and NPC1

Cholesterol metabolism in late endosomes is regulated by a number of cholesterol-binding and transporting proteins. Regulators also include lipids, such as lysobisphosphatidic acid (LBPA), which have been suggested to regulate cholesterol levels in LE (28). LBPA is exclusively

found in late endosomes, and we wondered whether it would localize to MLN64-positive, ORP1L-positive, or both LE compartments. We stained ORP1L- and MLN64-expressing cells with an antibody against LBPA (Fig. 6A). A fraction of both compartments labeled for LBPA. Cholesterol egresses from LE by the action of the Niemann Pick type C1 (NPC1) protein (16, 18) and acts upstream from ORP1L (10). We labeled cells for NPC1 and observed that NPC1 almost exclusively localized to ORP1L-positive vesicles while being absent from MLN64-positive late endosomes (Fig. 6B). Members of the ABCA family can pump cholesterol across membranes and localize to late endosomes and the PM (14, 29). Similar to MLN64, ABCA3 levels are high in lung (15). MLN64 and ABCA3 colocalized

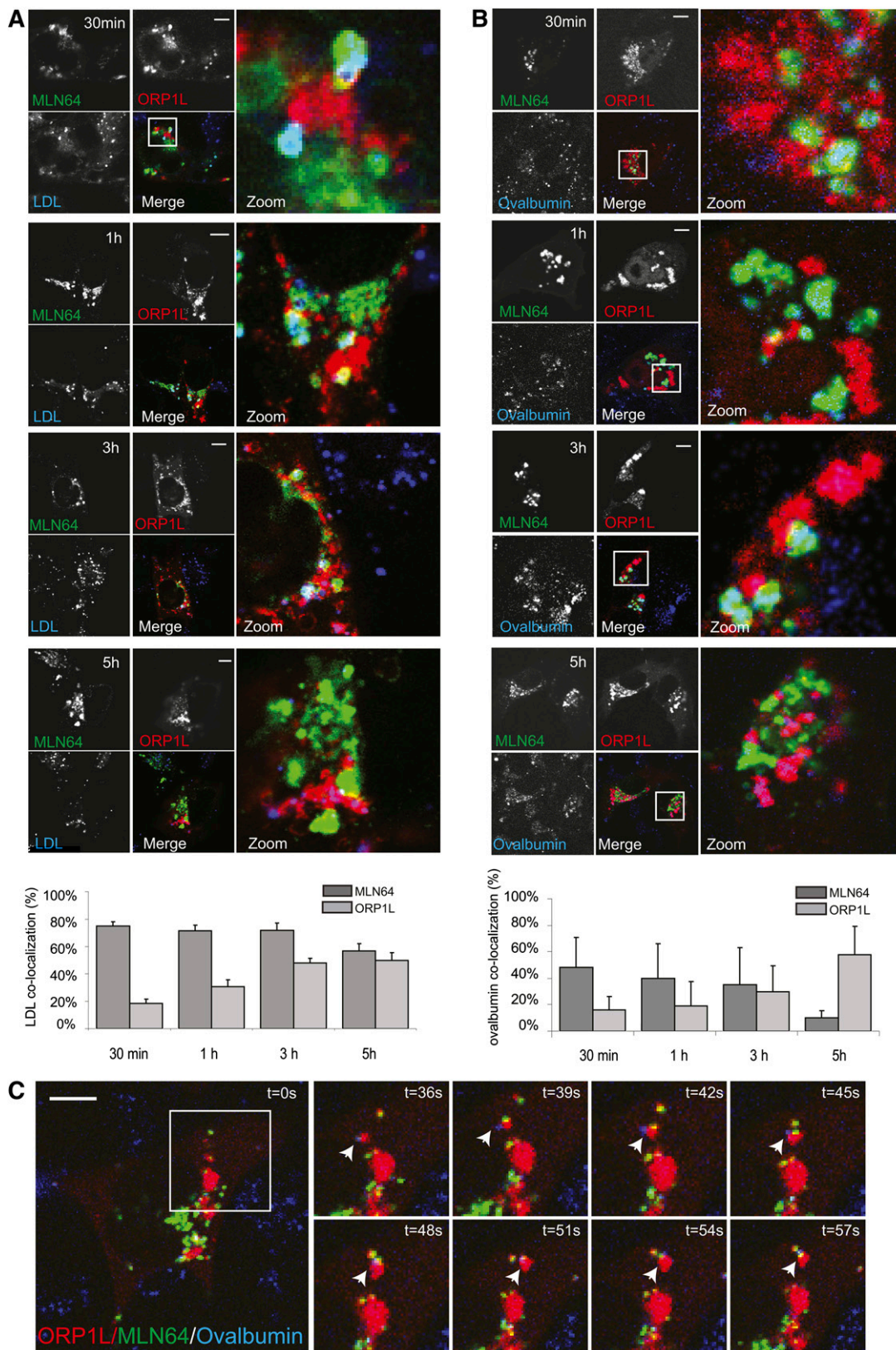


Fig. 5. Endocytic cargo passes from a MLN64-positive compartment to an ORP1L-positive compartment. (A) MelJuSo cells expressing MLN64-HA (green) and GFP-ORP1L (red) were incubated with Dil-LDL (blue) for 20 min (pulse) followed by a chase for indicated time points. Cells were then PFA fixed, permeabilized, and immunolabeled with anti-HA antibodies (green). Zoom-ins of merged pictures indicated. Scale bar: 10 μ m. Lower panel: Localization of Dil-LDL in HA-MLN64 or GFP-ORP1L vesicles was quantified using Manders coefficient [the percentage of blue pixels (LDL) overlapping with green (MLN64) or red (ORP1L) pixels]. $n > 25$. (B) MelJuSo cells expressing MLN64-YFP (green) and mRFP-ORP1L (red) were incubated with Cy5-ovalbumin (blue) for 20 min (pulse) followed by a chase for indicated time points. Zoom-ins of merged pictures indicated. Scale bar: 10 μ m. $n > 100$. Lower panel: Localization of Cy5-Ovalbumin in

on CD63-positive LE (Fig. 6C). Unlike NPC1, ABCA3 did not localize to ORP1L-positive LE (Fig. 6C). ORP1L vesicles represent cholesterol-rich endosomes (10) and overexpression of MLN64 also accumulates cholesterol in enlarged MLN64-positive compartments (4, 6–8, and data not shown). We wondered whether ABCA3 would also label vesicles accumulating cholesterol, like MLN64. We stained cells transfected with ORP1L and ABCA3 with filipin to detect free cholesterol and observed that the enlarged ABCA3-positive vesicles were also loaded with cholesterol (Fig. 6D). Our data indicate that MLN64 and ABCA3 are cholesterol-binding proteins on cholesterol-rich late endosomal compartments preceding later late endosomes in which NPC1 and ORP1L act together to coordinate cholesterol egress and late endosomal transport.

DISCUSSION

Egress of cholesterol from late endosomes requires the coordinated action of multiple cholesterol-binding and transporting molecules present on location. Here, we studied two proteins with cholesterol-sensing capabilities at the cytosolic leaflet of LE that regulate late endosomal dynamics, MLN64 and ORP1L. We show that these proteins locate to two late endosomal subpopulations. MLN64 is a membrane-integrated protein, and we show that it cycles with vesicles between LE and the PM and accumulates at the PM when endocytosis is blocked. This is similar to other late endosomal proteins, such as CD63, CD83, and HLA-DM (24, 25, 30–32). LDL and fluid-phase cargo first enter MLN64-positive LE before transport into ORP1L-positive LE, defining MLN64-positive LE as “early” late endosomes and ORP1L-positive LE as “late” late endosomes. ORP1L is recruited to LE endosomes by the small GTPase RAB7, which also recruits RILP to membranes. RILP recruits the dynein motor for minus-end transport to late endosomes, and overexpression of RILP induces strong clustering of LE vesicles near the microtubule organizing center (20). Conversely, silencing of RILP or a dominant-negative mutant of RILP (20) results in the scattering of endosomes as has been observed for MLN64 depletion, indicating that these may represent similar processes. However, we find that RILP and MLN64 are not on the same vesicles. This supports an observation by Holtta-Vuori and colleagues that RILP expression was unable to rescue the scattering of DiI-LDL-labeled endosomes in MLN64-depleted cells (8). Our data indicates that the CD63-containing LE can be subdivided into a subpopulation of MLN64-positive LE and a later subpopulation of late endosomes marked by RAB7-RILP-ORP1L.

The ORP1L- and MLN64-positive subpopulations displayed frequent contacts over longer periods of time (Fig. 3B and supplementary Movies I–III). We also observed a small fraction of LE containing both MLN64 and ORP1L. This can be expected when cargo is transferred from MLN64- to ORP1L-positive late endosomes by kiss-and-run events or, alternatively, by fusion of MLN64-containing LE with ORP1L-positive vesicles and fast sorting away from membrane-embedded MLN64. We have no evidence that MLN64 actively dissociates ORP1L from membranes. MLN64 has been proposed to promote endosomal tethering between endosomes via actin (8), and this might explain the interactions between ORP1L and MLN64 endosomes over long periods of time in living cells. If ORP1L- and MLN64-positive vesicles are able to (partially) fuse to exchange cargo, how is their spatial separation then achieved? A possible explanation might be fast tubulation and fission events that separate MLN64 and ORP1L vesicles quickly after they have formed a hybrid organelle. Tubulation and fission depend on the coordinated action of dynein and kinesin motors (32, 33), and ORP1L controls the recruitment of dynein motors to LE (10). ORP1L allows binding of the dynein motor under high LE cholesterol conditions, but it changes conformation when cholesterol is low in order to remove the dynein motor and allow for plus-end transport of LE by the kinesin motor (10). We observed that expression of an ORP1L mutant (ORP1L- Δ ORDPHDPHD) that stabilizes dynein motor binding to LE induced colocalization of MLN64 on ORP1L- Δ ORDPHDPHD-positive late endosomes. This might indicate that MLN64 and ORP1L vesicles are normally separated by the fission-opposing actions of kinesin and dynein motor activities, a process controlled by functional ORP1L. Similarly, this might explain why the expression of ORP1L- Δ ORD, which prevents dynein motor recruitment and therefore might disturb fission events, induces enlarged vesicles also positive for MLN64.

What is the role for the different subpopulations of late endosomes? If LE is separated in two subpopulations that precede each other and associate with different cholesterol-sensing proteins, they possibly have different roles in cholesterol trafficking, transfer, and distribution. ORP1L and the cholesterol transporter NPC1 localize on a subset of LE, whereas MLN64 and the cholesterol transporter ABCA3 localize on another LE subpopulation. The ORP1L/NPC1 vesicles might reflect a final stage in the internalization of LDL and transport of cholesterol from LE to the ER for further cellular distribution (10, 17, 19). Based on our observations and previous literature, we propose that the MLN64/ABCA3-positive late endosomes reflect an earlier stage in late endosomal maturation in which LDL is first hydrolyzed and free cholesterol can still be recycled back to the PM and/or cholesterol can be effluxed from

YFP-MLN64 or mRFP-ORP1L vesicles was quantified using Manders coefficient [the percentage of blue pixels (Ovalbumin) overlapping with green (MLN64) or red (ORP1L) pixels]. $n > 15$. (C) MeJuSo cells expressing MLN64-YFP (green) and ORP1L-mRFP (red) incubated with Cy5-ovalbumin (blue) for 20 min (pulse) followed by a chase for 3 h were imaged by time-lapse confocal microscopy. Merged, zoomed snapshots at different time points are shown (right panel). White arrowhead indicates MLN64-positive, ORP1L-positive, and Ovalbumin-positive vesicles interacting over prolonged times. Images correspond to supplementary Movie II.

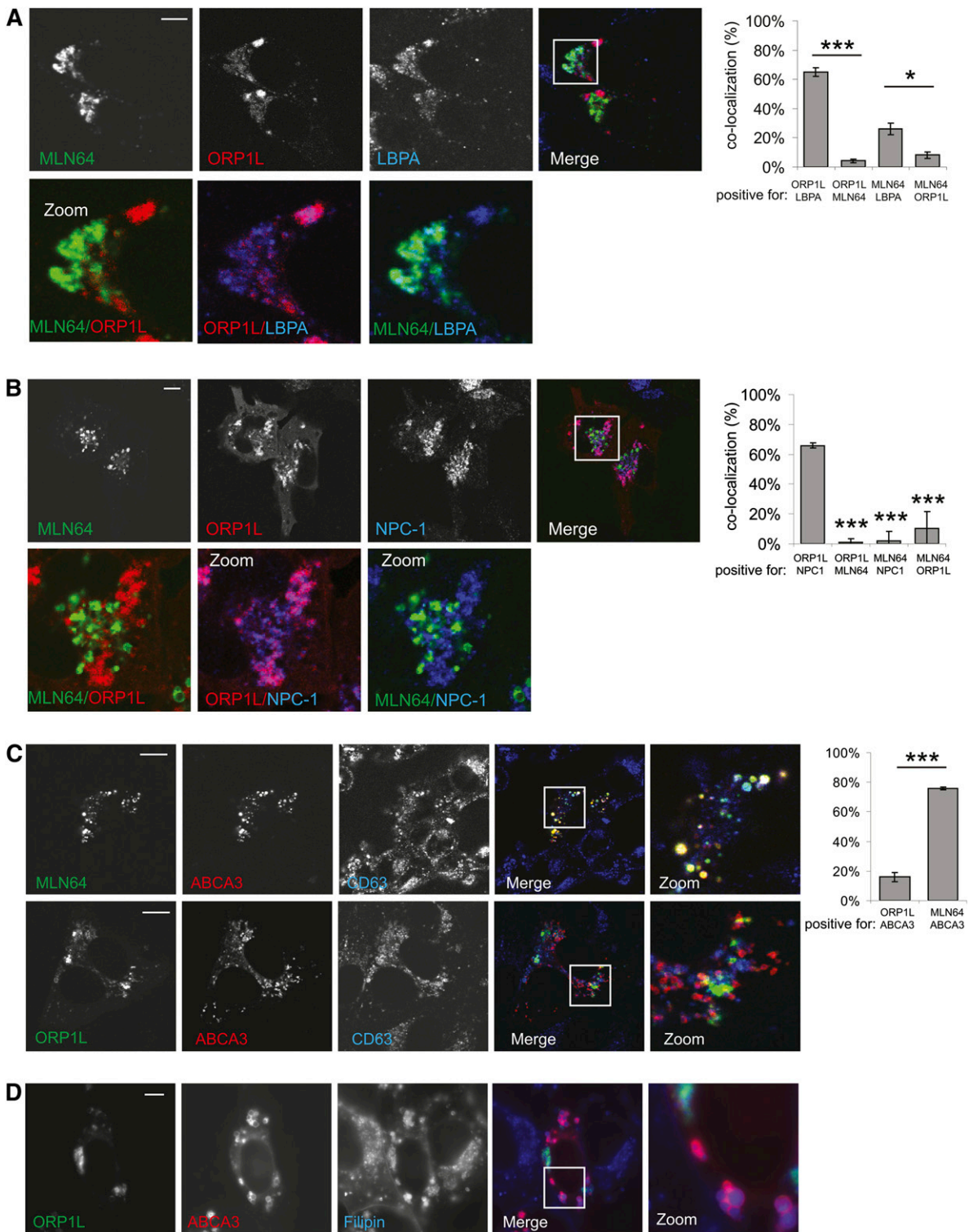


Fig. 6. Defining localization of late endosomal cholesterol-handling proteins. MelJuSo cells expressing MLN64-YFP (green) and m-RFP-ORP1L (red) were PFA fixed, permeabilized, and immunolabeled with anti-LBPA antibodies (A) or anti-NPC1 antibodies (B) and imaged by confocal microscopy. Zoom-ins of merged pictures indicated. Scale bar: 10 μ m. Right panel: Quantification of colocalization using Manders coefficient. Plotted is the percentage of signal A that is also positive for signal B for the indicated combinations. $n > 25$, $*P < 0.05$, $***P < 0.001$. (C) Upper panel: MelJuSo cells expressing MLN64-mRFP (green) and GFP-ABCA3 (red) were PFA fixed, permeabilized, and immunolabeled with anti-CD63 antibodies. Lower panel: MelJuSo cells expressing mRFP-ORP1L (green) and GFP-ABCA3 (red) were PFA fixed, permeabilized and immunolabeled with anti-CD63 antibodies. Right panel: Quantification of colocalization using Manders coefficient. Plotted is the percentage of signal A that is also positive for signal B for the indicated combinations. $n > 25$. (D) MelJuSo cells expressing MLN64-mRFP (green) and GFP-ABCA3 (red) were PFA fixed, permeabilized, and immunolabeled with Filipin for cholesterol staining followed by analysis by wide-field microscopy.

the cell via apolipoproteins. The exact function of ABCA3, which supposedly pumps lipids back into the lysosome (34), is unknown. ABCA3 might import cholesterol or other required lipids from lamellar-body biogenesis from other donor organelles into the LE (Fig. 7), or ABCA3 might be involved in the recycling of lipids from organelles, such as mitochondria, into LE where these then become available for redistribution to other compartments by NPC1-ORP5 (19) or Hrs (35). Alternatively, ABCA3 might be involved in the loading of free LE cholesterol or other lipids onto HDL or pulmonary surfactant lipoprotein particles, thereby decreasing LE lipid load. ABCA3 has previously been shown to be involved in early steps of late endosomal biogenesis (15), and both MLN64 and ABCA3 have higher expression in lung where ABCA3 has been shown to be important for the secretion of late endosomal lipids at the PM. Cholesterol destined for the mitochondria passes through the PM (36). MLN64 is involved in the egress of cholesterol from LE to mitochondria (4) in a process that is independent of NPC1 (7), indicating that MLN64 may be involved in the trafficking of cholesterol upstream of NPC1- and ORP1L-containing late endosomes as an additional step for LE cholesterol export. The existence of two consecutive late endosomal compartments,

each different in cholesterol handling to donor compartments, might explain earlier observations that one pool of LE cholesterol is quickly transported to the plasma membrane while another pool of LE cholesterol is transported to the ER more slowly (2, 3, 18) and that NPC2 can function in cholesterol delivery to mitochondria independent of NPC1 (37).

Increased levels of MLN64, such as observed in breast and prostate cancer (38–41), might stimulate the transfer of cholesterol from LE to mitochondria where steroidogenesis occurs to produce hormones, such as progesterone, estrogen, and testosterone, required for tumor growth. Conversely, this would result in a decrease of cholesterol traffic toward “later” late endosomes and the ER. Indeed, overexpression of MLN64 in macrophages increases cholesterol efflux and prevents increases in ER cholesterol esterification in response to acetylated LDL inducing an antiatherogenic lipid phenotype (42).

In summary, MLN64 and ORP1L define two subpopulations of late endosomes that precede each other in maturation stages. The cholesterol influx pump ABCA3 is present on MLN64-positive “early” late endosomes and the cholesterol effluxer NPC1 is present on ORP1L-positive “late” late endosomes (Fig. 7). MLN64/ABCA3 vesicles can

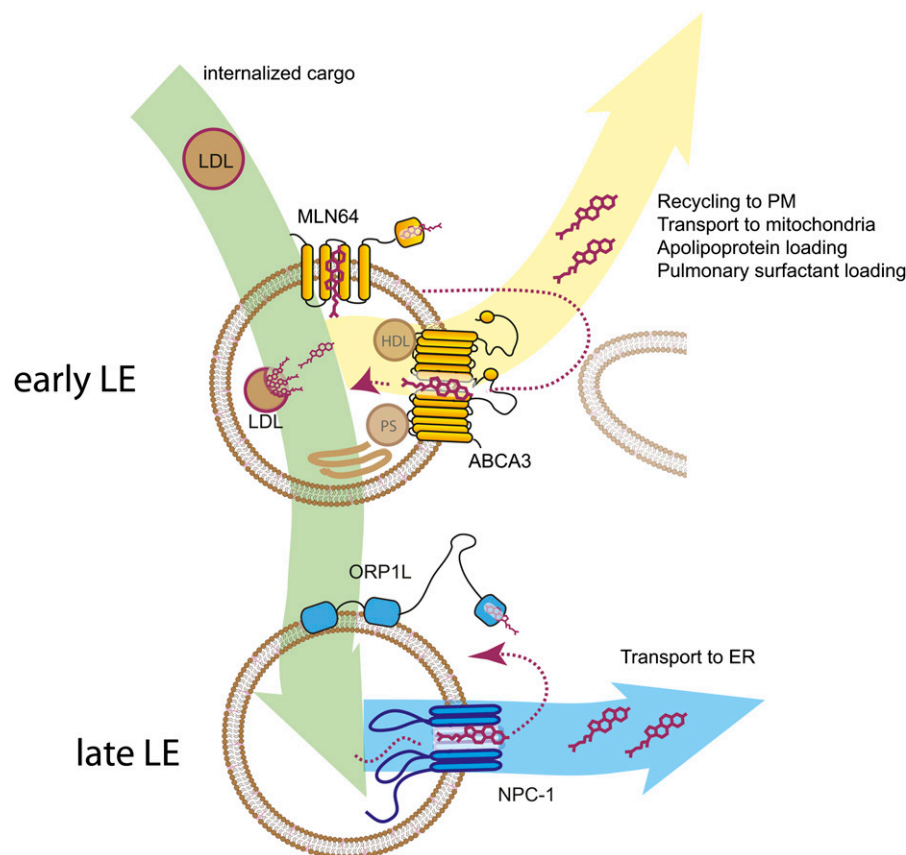



Fig. 7. Model of cholesterol dynamics in MLN64/ABCA3 and ORP1L/NPC1 vesicles. LDL particles derived from internalization enter via early endosomes into a MLN64/ABCA3-positive “early” late endosome where LDL can be hydrolyzed and cholesterol released. From here, cholesterol can be recycled to the plasma membrane by the action of MLN64/ABCA3 vesicles. Alternatively, cholesterol is further transported to ORP1L/NPC1-positive “late” LE that can contact the ER to export cholesterol from the LE to the ER for further distribution throughout the cell.

cycle to the plasma membrane, whereas ORPIL/NPCI vesicles reflect a later stage in endocytosis. Together our findings indicate that these late endosomal subpopulations define different states of cholesterol handling. 

The authors thank V. Olkkonen and F Alpy for providing reagents.

REFERENCES

- Ikonen, E. 2008. Cellular cholesterol trafficking and compartmentalization. *Nat. Rev. Mol. Cell Biol.* **9**: 125–138.
- Neufeld, E. B., A. M. Cooney, J. Pitha, E. A. Dawidowicz, N. K. Dwyer, P. G. Pentchev, and E. J. Blanchette-Mackie. 1996. Intracellular trafficking of cholesterol monitored with a cyclodextrin. *J. Biol. Chem.* **271**: 21604–21613.
- Lange, Y., J. Ye, and J. Chin. 1997. The fate of cholesterol exiting lysosomes. *J. Biol. Chem.* **272**: 17018–17022.
- Zhang, M., P. Liu, N. K. Dwyer, L. K. Christenson, T. Fujimoto, F. Martinez, M. Comly, J. A. Hanover, E. J. Blanchette-Mackie, and J. F. Strauss 3rd. 2002. MLN64 mediates mobilization of lysosomal cholesterol to steroidogenic mitochondria. *J. Biol. Chem.* **277**: 33300–33310.
- Mobius, W., E. van Donselaar, Y. Ohno-Iwashita, Y. Shimada, H. F. Heijnen, J. W. Slot, and H. J. Geuze. 2003. Recycling compartments and the internal vesicles of multivesicular bodies harbor most of the cholesterol found in the endocytic pathway. *Traffic*. **4**: 222–231.
- Alpy, F., M. E. Stoeckel, A. Dierich, J. M. Escola, C. Wendling, M. P. Chenard, M. T. Vanier, J. Gruenberg, C. Tomasetto, and M. C. Rio. 2001. The steroidogenic acute regulatory protein homolog MLN64, a late endosomal cholesterol-binding protein. *J. Biol. Chem.* **276**: 4261–4269.
- Charman, M., B. E. Kennedy, N. Osborne, and B. Karten. 2010. MLN64 mediates egress of cholesterol from endosomes to mitochondria in the absence of functional Niemann-Pick Type C1 protein. *J. Lipid Res.* **51**: 1023–1034.
- Holttä-Vuori, M., F. Alpy, K. Tanhuanpää, E. Jokitalo, A. L. Mutka, and E. Ikonen. 2005. MLN64 is involved in actin-mediated dynamics of late endocytic organelles. *Mol. Biol. Cell.* **16**: 3873–3886.
- Johansson, M., N. Rocha, W. Zwart, I. Jordens, L. Janssen, C. Kuijl, V. M. Olkkonen, and J. Neeffjes. 2007. Activation of endosomal dynein motors by stepwise assembly of Rab7-RILP-p150Glued, ORPIL, and the receptor betalll spectrin. *J. Cell Biol.* **176**: 459–471.
- Rocha, N., C. Kuijl, R. van der Kant, L. Janssen, D. Houben, H. Janssen, W. Zwart, and J. Neeffjes. 2009. Cholesterol sensor ORPIL contacts the ER protein VAP to control Rab7-RILP-p150 Glued and late endosome positioning. *J. Cell Biol.* **185**: 1209–1225.
- Johansson, M., M. Lehto, K. Tanhuanpää, T. L. Cover, and V. M. Olkkonen. 2005. The oxysterol-binding protein homologue ORPIL interacts with Rab7 and alters functional properties of late endocytic compartments. *Mol. Biol. Cell.* **16**: 5480–5492.
- van der Kant, R., A. Fish, L. Janssen, H. Janssen, S. Krom, N. Ho, T. Brummelkamp, J. Carette, N. Rocha, and J. Neeffjes. Late endosomal transport and tethering are coupled processes controlled by RILP and the cholesterol sensor ORPIL. *J. Cell Sci.* Epub ahead of print. <http://www.ncbi.nlm.nih.gov/pubmed/23729732>.
- Uusi-Rauva, K., A. Kyttälä, R. van der Kant, J. Vesa, K. Tanhuanpää, J. Neeffjes, V. M. Olkkonen, and A. Jalanko. 2012. Neuronal ceroid lipofuscinosis protein CLN3 interacts with motor proteins and modifies location of late endosomal compartments. *Cell. Mol. Life Sci.* **69**: 2075–2089.
- Beers, M. F., A. Hawkins, H. Shuman, M. Zhao, J. L. Newitt, J. A. Maguire, W. Ding, and S. Mulugeta. 2011. A novel conserved targeting motif found in ABCA transporters mediates trafficking to early post-Golgi compartments. *J. Lipid Res.* **52**: 1471–1482.
- Cheong, N., H. Zhang, M. Madesh, M. Zhao, K. Yu, C. Dodia, A. B. Fisher, R. C. Savani, and H. Shuman. 2007. ABCA3 is critical for lamellar body biogenesis in vivo. *J. Biol. Chem.* **282**: 23811–23817.
- Naureckiene, S., D. E. Sleat, H. Lackland, A. Fensom, M. T. Vanier, R. Wattiaux, M. Jadot, and P. Lobel. 2000. Identification of HE1 as the second gene of Niemann-Pick C disease. *Science*. **290**: 2298–2301.
- Mukherjee, S., and F. R. Maxfield. 2004. Lipid and cholesterol trafficking in NPC. *Biochim. Biophys. Acta.* **1685**: 28–37.
- Underwood, K. W., B. Andemariam, G. L. McWilliams, and L. Liscum. 1996. Quantitative analysis of hydrophobic amine inhibition of intracellular cholesterol transport. *J. Lipid Res.* **37**: 1556–1568.
- Du, X., J. Kumar, C. Ferguson, T. A. Schulz, Y. S. Ong, W. Hong, W. A. Prinz, R. G. Parton, A. J. Brown, and H. Yang. 2011. A role for oxysterol-binding protein-related protein 5 in endosomal cholesterol trafficking. *J. Cell Biol.* **192**: 121–135.
- Vennegoor, C., and P. Rumke. 1986. Circulating melanoma-associated antigen detected by monoclonal antibody NK1/C-3. *Cancer Immunol. Immunother.* **23**: 93–100.
- Jordens, I., M. Fernandez-Borja, M. Marsman, S. Dusseljee, L. Janssen, J. Calafat, H. Janssen, R. Wubbolts, and J. Neeffjes. 2001. The Rab7 effector protein RILP controls lysosomal transport by inducing the recruitment of dynein-dynactin motors. *Curr. Biol.* **11**: 1680–1685.
- Wu, C., C. Orozco, J. Boyer, M. Leglise, J. Goodale, S. Batalov, C. L. Hodge, J. Haase, J. Janes, J. W. 3rd Huss, and A. I. Su. 2009. BioGPS: an extensible and customizable portal for querying and organizing gene annotation resources. *Genome Biol.* **10**: R130.
- Schnell, U., F. Dijk, K. A. Sjollem, and B. N. Giepmans. 2012. Immunolabeling artifacts and the need for live-cell imaging. *Nat. Methods.* **9**: 152–158.
- Pols, M. S., and J. Klumperman. 2009. Trafficking and function of the tetraspanin CD63. *Exp. Cell Res.* **315**: 1584–1592.
- Klein, E., S. Koch, B. Borm, J. Neumann, V. Herzog, N. Koch, and T. Bieber. 2005. CD83 localization in a recycling compartment of immature human monocyte-derived dendritic cells. *Int. Immunol.* **17**: 477–487.
- Lee, A., D. W. Frank, M. S. Marks, and M. A. Lemmon. 1999. Dominant-negative inhibition of receptor-mediated endocytosis by a dynamin-1 mutant with a defective pleckstrin homology domain. *Curr. Biol.* **9**: 261–264.
- Kobuna, H., T. Inoue, M. Shibata, K. Gengyo-Ando, A. Yamamoto, S. Mitani, and H. Arai. 2010. Multivesicular body formation requires OSBP-related proteins and cholesterol. *PLoS Genet.* **6**: pii: e1001055.
- Matsuo, H., J. Chevallier, N. Mayran, I. Le Blanc, C. Ferguson, J. Fauré, N. S. Blanc, S. Matile, J. Dubochet, R. Sadoul, R. G. Parton, F. Vilbois, and J. Gruenberg. 2004. Role of LBPA and Alix in multivesicular liposome formation and endosome organization. *Science*. **303**: 531–534.
- Schaller-Bals, S., S. R. Bates, K. Notarfrancesco, J. Q. Tao, A. B. Fisher, and H. Shuman. 2000. Surface-expressed lamellar body membrane is recycled to lamellar bodies. *Am. J. Physiol. Lung Cell. Mol. Physiol.* **279**: L631–L640.
- Hoorn, T., P. Paul, L. Janssen, H. Janssen, and J. Neeffjes. 2012. Dynamics within tetraspanin pairs affect MHC class II expression. *J. Cell Sci.* **125**: 328–339.
- Copier, J., M. J. Kleijmeer, S. Ponnambalam, V. Oorschot, P. Potter, J. Trowsdale, and A. Kelly. 1996. Targeting signal and subcellular compartments involved in the intracellular trafficking of HLA-DMB. *J. Immunol.* **157**: 1017–1027.
- Mrakovic, A., J. G. Kay, W. Furuya, J. H. Brumell, and R. J. Botelho. 2012. Rab7 and Arl8 GTPases are necessary for lysosome tubulation in macrophages. *Traffic*. **13**: 1667–1679.
- Soppina, V., A. K. Rai, A. J. Ramaia, P. Barak, and R. Mallik. 2009. Tug-of-war between dissimilar teams of microtubule motors regulates transport and fission of endosomes. *Proc. Natl. Acad. Sci. USA.* **106**: 19381–19386.
- van Meer, G., D. Halter, H. Sprong, P. Somerharju, and M. R. Egmond. 2006. ABC lipid transporters: extruders, flippases, or floppase activators? *FEBS Lett.* **580**: 1171–1177.
- Du, X., A. S. Kazim, A. J. Brown, and H. Yang. 2012. An essential role of Hrs/Vps27 in endosomal cholesterol trafficking. *Cell Rep.* **1**: 29–35.
- Lange, Y., T. L. Steck, J. Ye, M. H. Lanier, V. Molugu, and D. Ory. 2009. Regulation of fibroblast mitochondrial 27-hydroxycholesterol production by active plasma membrane cholesterol. *J. Lipid Res.* **50**: 1881–1888.
- Kennedy, B. E., M. Charman, and B. Karten. 2012. Niemann-Pick Type C2 protein contributes to the transport of endosomal cholesterol to mitochondria without interacting with NPC1. *J. Lipid Res.* **53**: 2632–2642.
- Kauraniemi, P., M. Barlund, O. Monni, and A. Kallioniemi. 2001. New amplified and highly expressed genes discovered in the ERBB2 amplicon in breast cancer by cDNA microarrays. *Cancer Res.* **61**: 8235–8240.

39. Moog-Lutz, C., C. Tomasetto, C. H. Regnier, C. Wendling, Y. Lutz, D. Muller, M. P. Chenard, P. Basset, and M. C. Rio. 1997. MLN64 exhibits homology with the steroidogenic acute regulatory protein (STAR) and is over-expressed in human breast carcinomas. *Int. J. Cancer*. **71**: 183–191.
40. Alpy, F., A. Boulay, C. Moog-Lutz, K. L. Andarawewa, S. Degot, I. Stoll, M. C. Rio, and C. Tomasetto. 2003. Metastatic lymph node 64 (MLN64), a gene overexpressed in breast cancers, is regulated by Sp/KLF transcription factors. *Oncogene*. **22**: 3770–3780.
41. Vinatzer, U., B. Dampier, B. Streubel, M. Pacher, M. J. Seewald, C. Stratowa, K. Kaserer, and M. Schreiber. 2005. Expression of HER2 and the coamplified genes GRB7 and MLN64 in human breast cancer: quantitative real-time reverse transcription-PCR as a diagnostic alternative to immunohistochemistry and fluorescence in situ hybridization. *Clin. Cancer Res.* **11**: 8348–8357.
42. Borthwick, F., A. M. Allen, J. M. Taylor, and A. Graham. 2010. Overexpression of STARD3 in human monocyte/macrophages induces an anti-atherogenic lipid phenotype. *Clin. Sci. (Lond.)*. **119**: 265–272.